Development of Composite Sandwich Bonded Longitudinal Joints for Space Launch Vehicle Structures

David W. Sleight[1]
NASA Langley Research Center, Hampton, VA 23681, USA

Kenneth N. Segal[2]
NASA Goddard Space Flight Center, Greenbelt, MD 20771, USA

William E. Guin[3], Matthew R. McDougal[4], Casey C. Wolfe[5], Mallory M. Johnston[6]
NASA Marshall Space Flight Center, Huntsville, AL 35812, USA

and
Sandi G. Miller[7]
NASA Glenn Research Center, Cleveland, OH 44135, USA

The NASA Composite Technology for Exploration (CTE) Project is developing and demonstrating critical composite technologies with a focus on composite bonded joints; incorporating materials, design/analysis, manufacturing, and tests that utilize NASA's expertise and capabilities. The project has goals of advancing composite technologies and providing lightweight structures to support future NASA exploration missions. In particular, the CTE project will demonstrate weight-saving, performance-enhancing composite bonded joint technology for Space Launch System (SLS)-scale composite hardware. Advancements from the CTE project may be incorporated as future block upgrades for SLS structural components. This paper discusses the details of the development of a composite sandwich bonded longitudinal joint for a generic space launch vehicle structure called the *CTE Point Design.* The paper includes details of the design, analysis, materials, manufacturing, and testing of sub-element joint test articles to test the capability of the joint design. The test results show that the composite longitudinal bonded joint design significantly exceeds the design loads with a 2.0 factor of safety. Analysis pre-test failure predictions for all sub-element bonded joint test coupons were all within 10% of the average test coupon failure load. This testing and analysis provides confidence in the potential use of composite bonded joints for future launch vehicle structures.

I. Introduction

The NASA Composite Technology for Exploration (CTE) Project is developing and demonstrating critical composite technologies with a focus on joints; incorporating materials, design/analysis, manufacturing, and tests that utilize NASA expertise and capabilities. The CTE project kicked off in 2017 and is a multi-Center project led by Marshall Space Flight Center (MSFC) and supported by Glenn Research Center (GRC), Goddard Space Flight Center (GSFC), Kennedy Space Center (KSC), and the Langley Research Center (LaRC). The project has been funded by the Game Changing Development (GCD) Program in the Space Technology Mission Directorate (STMD) and the Spacecraft Payload Integration and Evolution (SPIE) Office in the Space Launch System (SLS) Program. The project has goals of advancing composite technologies and providing lightweight structures to support future NASA

[1] Aerospace Engineer, Structural and Thermal Systems Branch, AIAA Senior Member.
[2] Aerospace Engineer, Mechanical Engineering Branch.
[3] Materials and Process Engineer, Advanced Manufacturing Branch.
[4] NDE Engineer, Damage Tolerance Assessment Branch.
[5] Materials Engineer, Advanced Manufacturing Branch.
[6] Deputy Project Manager, Space Technology Development Branch.
[7] Chemical Engineer, Ceramic and Polymer Composites Branch.

exploration missions. In particular, the CTE project has plans to demonstrate weight-saving, performance-enhancing composite bonded joint technology for Space Launch System (SLS)-scale composite hardware. Advancements from the CTE project may be incorporated as future block upgrades for SLS structural components. Further, the project will advance the state of the art in the detailed analyses of composite bonded joints for joint failure prediction. The CTE project builds upon composite design and manufacturing knowledge obtained from earlier NASA programs [1-5].

For the first two years of the project, the CTE project focused on the development of composite longitudinal bonded joint technologies for conical structures such as the SLS Payload Attach Fitting (PAF) due to challenging joint geometries and loads compared to cylindrical jointed structures. As shown in Figure 1, the conical PAF resides within the Universal Stage Adapter (USA) in the Exploration Upper Stage (EUS) of the SLS. Payloads for the SLS are mounted atop the PAF. Alternative SLS configurations also allow for payload only missions with a fairing instead of the USA. The diameter of the conical PAF at its bottom circumferential joint is 8.4 meters, making the PAF too large to manufacture as one piece in all but the largest autoclaves; therefore, the PAF is being designed to be manufactured in eight sections connected with longitudinal joints (see Figure 1). As part of this focus on longitudinal bonded joint technologies for conical structures, the CTE project worked with the SLS/PAF team to develop a generic PAF design called the *CTE Point Design* with a goal of advancing manufacturing and analysis prediction technologies for composite longitudinal bonded joints. The CTE project has several key performance parameters (KPP) for measuring the success of the project which are listed in Table 1.

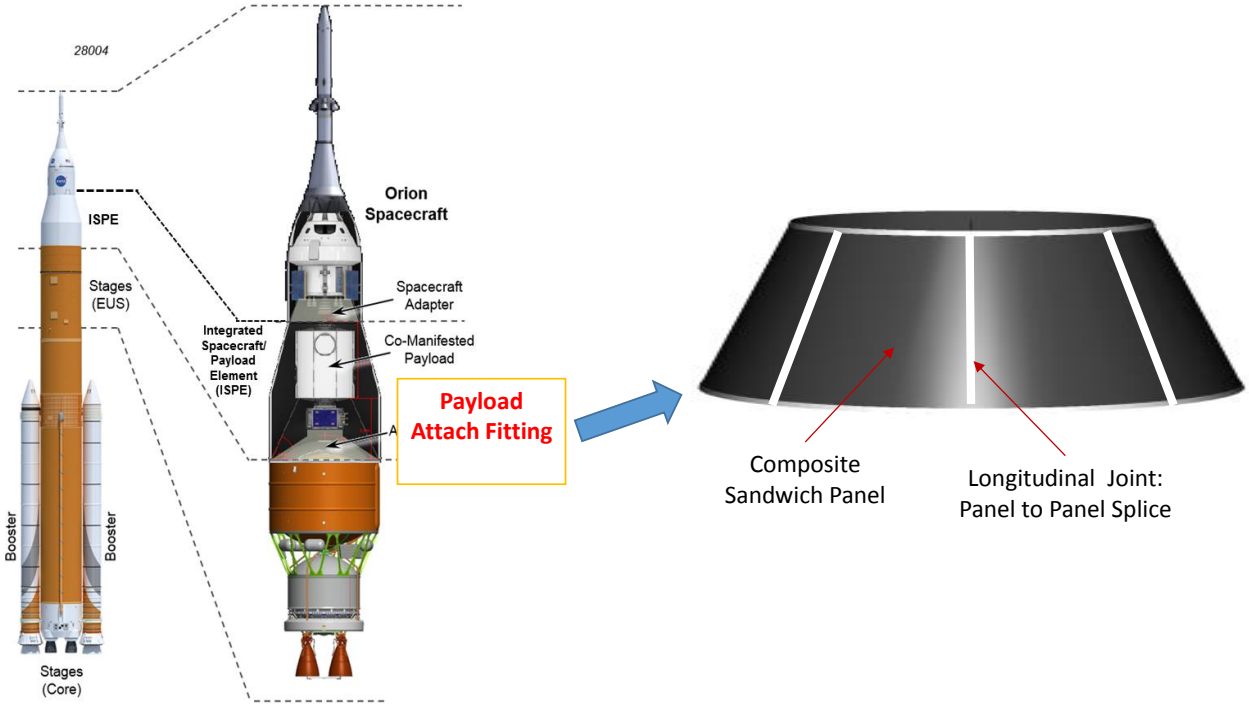

https://www.nasa.gov/exploration/systems/sls/multimedia/images.html

Figure 1 Exploded view of SLS showing PAF.

Table 1 CTE Project Key Performance Parameters.

Key Performance Parameters			
Performance Parameter	State of the Art	Threshold Value	Project Goal
KPP-1. Accurate Pre-test Prediction of Bonded Joint Failure Load based on new analytical techniques.	Predicted bonded joint failure load within ±25 percent of mean test failure load.	Demonstrate predicted bonded joint failure load within ±15 percent of mean test failure load.	Demonstrate predicted bonded joint failure load within ±5 percent of mean test failure load.
KPP-2, Reduced discontinuity factor of safety for joints in primary load path for an SLS-like composite structure. (Discontinuity Factor of Safety = Ǝ * 2.0, where Ǝ is a risk reduction factor based on new analytical techniques and test data)	2.0 (Current Requirement)	1.8 (tailored approach - prototype)	1.4 (tailored approach - prototype)
KPP-3. Reduce part count associated with joints in primary load path for 8.4m diameter scale composite structures.	100% metal/bolted joint	25% reduction in part count	50% reduction in part count
KPP-4. Reduce weight associated with joints in primary load path for 8.4m diameter scale composite structures. (example: reduction from 3 lb/ft joint length to much lower weight per linear foot bondline length)	Metal/bolted joint	15% reduction from metal or bolted joint	25% reduction from metal or bolted joint

The CTE team developed a technology plan (See Figure 2) for advancing the technology of composite longitudinal bonded joints for a generic space launch vehicle structure. The team leveraged the materials used in previous projects and chose materials that were scalable to large-scale launch vehicle structures. Material characterization tests were performed to obtain the necessary material properties needed for the structural analysis models for joint failure predictions. The team performed preliminary analyses to size the composite sandwich acreage panels and determine the geometry of the generic PAF conical structure. The final generic PAF design was referred to as the *CTE Point Design*. The project leveraged joint studies in previous projects to select a double-lap composite bonded splice joint for the CTE project based on its figures of merit. Next, preliminary and detailed joint analyses were performed to determine the details of the longitudinal double-lap composite bonded splice joint design. Afterwards, a joint manufacturing process development effort was undertaken to optimize the surface preparation process needed for a consistent bonded joint. Non-Destructive Evaluation (NDE) methods were investigated for the post bond inspection to determine the suitability of the NDE method for detecting the bond quality. Thereafter, composite sandwich longitudinal joint panels were fabricated and machined into joint sub-element test specimens according to a test matrix established by the project. The test matrix called for the joint specimens to be tested under various loading configurations including axial compression, hoop compression, and hoop tension to assess the structural performance of the CTE longitudinal composite sandwich bonded joint design and to validate the structural models for joint failure prediction.

In this paper, the details of the development of a composite sandwich bonded longitudinal joint for a generic space launch vehicle structure called the *CTE Point Design* will be described including the design, analysis, materials, manufacturing, and testing. The paper is organized as follows. Section II provides an overview of the materials chosen for the project. Section III discusses the structural design and analysis process used to select the longitudinal joint design. It also discusses the design and analysis of longitudinal joint sub-element test articles to test the capability of the joint design. Section IV presents details of the CTE manufacturing process used to fabricate the CTE down-selected composite sandwich longitudinal joint panels. Section V presents the longitudinal joint sub-element test results. Finally, Section VI presents a summary of the CTE longitudinal bonded joint development effort.

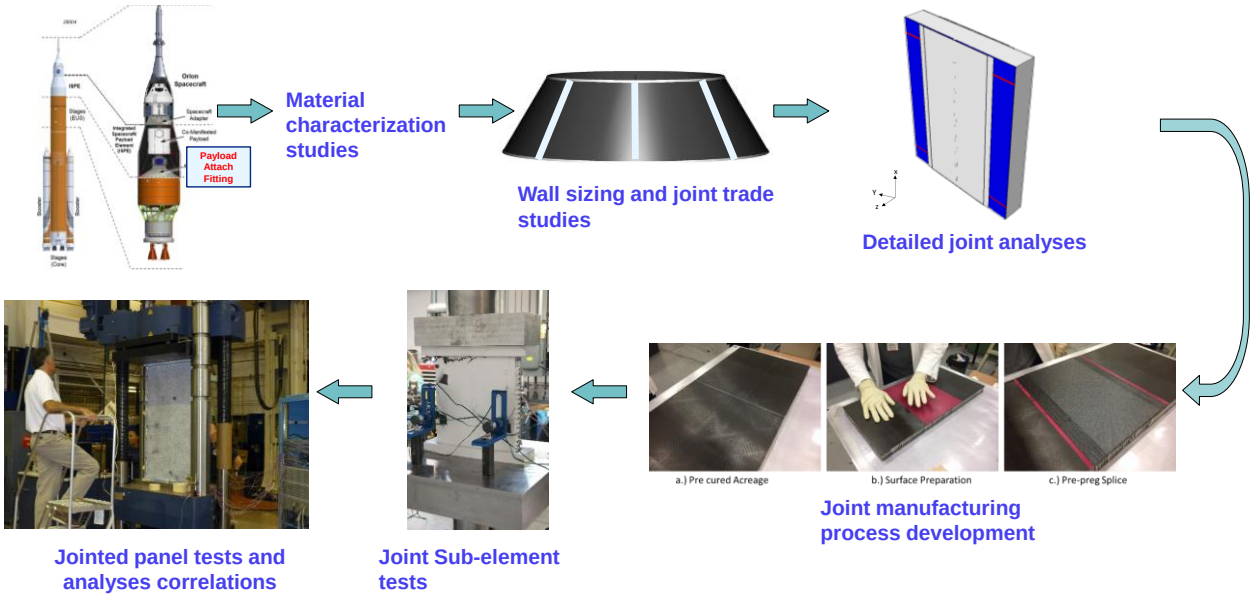

Figure 2 CTE Technology Plan for Joint Development.

II. Materials

Composite materials for the CTE project were chosen based on a number of considerations including processability, performance, and the availability of material properties databases. The material selected for the composite sandwich acreage panels for the face-sheets was IM7/8552-1 with a fiber areal weight (FAW) of 190 g/m^2 and a resin content of 35 ±2 wt%. The IM7/8552-1 carbon fiber and epoxy prepreg was a variant of the IM7/8552 prepreg used to populate a National Center for Advanced Materials Performance (NCAMP) database [6,7]. The 8552-1 variant demonstrates a lower tack, facilitating fiber placement as compared to the baseline 8552 based prepreg. As data for the 8552 form of the material is available through the NCAMP database, the project adopted an accelerated building block approach in the form of an equivalency test matrix, to reduce schedule-related risk [8]. The parent tape form of the prepreg was manufactured by the Hexcel Corporation* in Salt Lake City, UT., where the internal specification HS-AD-971B was followed. The CTE project kicked off in 2017 with remaining IM7/8552-1 prepreg from a previous project called the Composites for Exploration Upper Stage (CEUS) Project [3]. For the use of the IM7/8552-1 prepreg by the CTE Project, the material had to be recertified (due to its age) through an in-house defined set of pass/fail criteria and then evaluated for equivalency to the NCAMP database [6]. Panels for recertification and equivalency tests were fiber placed at NASA's MSFC and LaRC. Recertification and equivalency testing was performed at the National Institute for Aviation Research (NIAR) and at NASA's GRC and MSFC. For the sandwich panel core, a 3.1-lb/ft^3, perforated aluminum core (5056) with (3/16-in.) hexagonal cell sizes was chosen. The doubler material used within the CTE project was 5320-1/PW T650 3K epoxy and carbon fiber woven prepreg from Solvay Industries*. This material was chosen as material properties were available within the NCAMP database, and therefore prepreg fabrication followed NCAMP specification NMS 532/6. This specification calls for a FAW of 193 g/m^2 and a resin content of 37 wt%. The plain weave fabric utilized 3K fiber tow size. For both the acreage and doubler material, coupon data not available within the NCAMP database was tested by the project as required. Additional testing was conducted to obtain fracture toughness value material properties for the fabric material and stiffness property data for the film adhesive for the analysis models used to predict joint failure.

The adhesive used in the composite bonded joint was Solvay's FM209-1M film adhesive which was compatible with the out-of-autoclave cure process planned for the joint manufacturing. Tensile tests of the film adhesive were performed at the National Institute of Aviation Research (NIAR) following ASTM standard D638, method 1, and the adhesive shear strength tested by Element Labs following ASTM Standard D5656.

* The use of trademarks or names of manufacturers in this report is for accurate reporting and does not constitute an official endorsement, either expressed or implied, of such products or manufacturers by the National Aeronautics and Space Administration.

III. CTE Structural Analysis and Design

The CTE project leveraged joint trade studies for longitudinal joints from past NASA projects, the Advanced Composite Technology (ACT) Project which ran from 2008-2010, the Lightweight Spacecraft Structures & Materials (LSSM) Project which ran from 2010-2011, and the CEUS project which ran from 2014-2016. A double-lap composite bonded joint was selected as the most advantageous longitudinal joint to advance for the CTE project. The joint selection was based on an assessment of figures of merit for mass, damage tolerance, inspectability, cost, design/analysis uncertainty, and producability. The qualitative results of the assessment are shown in Table 2 with all rankings compared to a metallic bolted doubler joint with bushings chosen as the benchmark. The down-selected composite bonded doubler joint, as shown in Figure 3 joins six segmented composite sandwich panels together by bonding a prepreg T650/5320-1 fabric doubler using FM209-1M adhesive. A design assumption was that individual panel removal in the final assembled structure would not be possible. Another assumption was that uniform transfer of load was assumed into the joints.

Table 2 CTE Longitudinal Joint Downselect Assessment

Metric Information		*Conceptual Solutions*					
		Benchmark	A	B	C	D	E
Figures of Merit		Metallic Doubler Bolted (Bushings)	Metallic Clevis Bolted (HD Core)	Composite Doubler Bolted (Bushings)	Composite Doubler Bolted (HD Core)	Composite Doubler (Bonded)	Composite Durable Redundant Joint
Basic Mass		Same	Worse	Better	Worse	Better	Better
Structural Integrity / Damage Tolerance		Same	Same	Worse	Worse	Same	Better
Inspectability		Same	Better	Same	Better	Better	Worse
Minimum Recurring Cost		Same	Better	Worse	Better	Better	Same
Minimum Non Recurring Cost		Same	Same	Same	Same	Better	Same
Minimal Development Cost		Same	Same	Worse	Worse	Same	Same
Design/Analysis Uncertainty		Same	Same	Same	Same	Same	Same
Producability/Complexity		Same	Better	Same	Better	Better	Worse

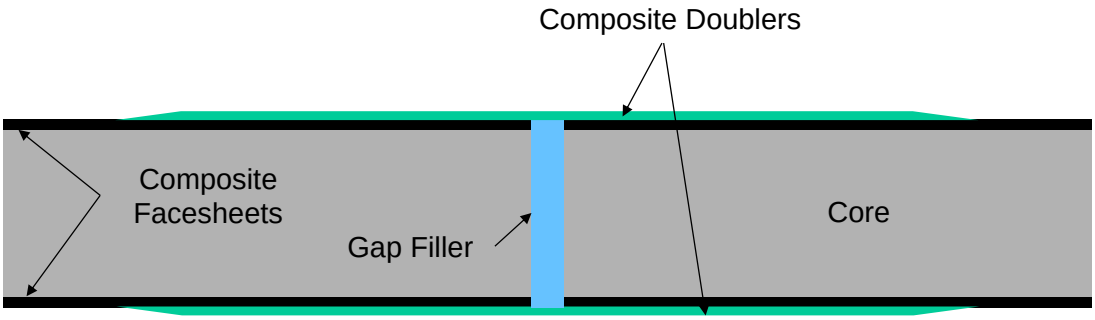

Figure 3 CTE Down-Selected Longitudinal Joint.

Next the project worked with the SLS PAF team to develop generic PAF conical geometries for a range of cone heights and angles along with generic loadings applicable to space launch vehicle structures. The loads were derived from the launch accelerations for a Delta IV rocket [9] with a 10-metric ton payload and are given below in Section A. The acreage panels chosen were a sandwich construction with a Plascore 3.1-lb/ft^3 aluminum core (5056) with (3/16-in.) hexagonal cells and IM7/8552-1 quasi-isotropic graphite/epoxy facesheets. The material for the doubler plates was a T650/5320-1 epoxy and carbon fiber woven prepreg fabric from Solvay Industries. Details of the sizing and analysis used to establish a structure called the *CTE Point Design* is discussed in Section B.

A. CTE Structural Requirements and Loads to Establish *CTE Point Design* Geometry

Factors of safety (FS) requirements are given below for composite and metallic structures from the NASA Standard 5001-B document [10]. A shell bucking knockdown factor of 0.5 was assumed for the CTE conical structure. This was based on a CTE buckling study [11] for conical shells similar to geometry of the CTE structure that showed

a knockdown factor of 0.50 was still conservative but not as overly conservative based on the NASA SP-8019 report published in 1968 [12].

- Composites: Ultimate 1.5, Limit 1.0, Discontinuity, 2.0
- Metallic: Ultimate 1.4, Yield 1.25

The following information was provided by the SLS PAF team to help the CTE project in developing or maturing bonded joint technologies. The loads were developed from Delta 4 accelerations for a 10-metric ton payload at a distance of 7 feet above the separation plane (top of CTE) with a center of gravity (CG) lateral offset of 5 inches. The loads are bounding loading conditions that if addressed should prove applicable to NASA launch vehicle structure applications and are shown in Figure 4. Figure 5 shows the applied loads on the CTE structure. Figure 4 also shows the range of CTE geometries for different configurations.

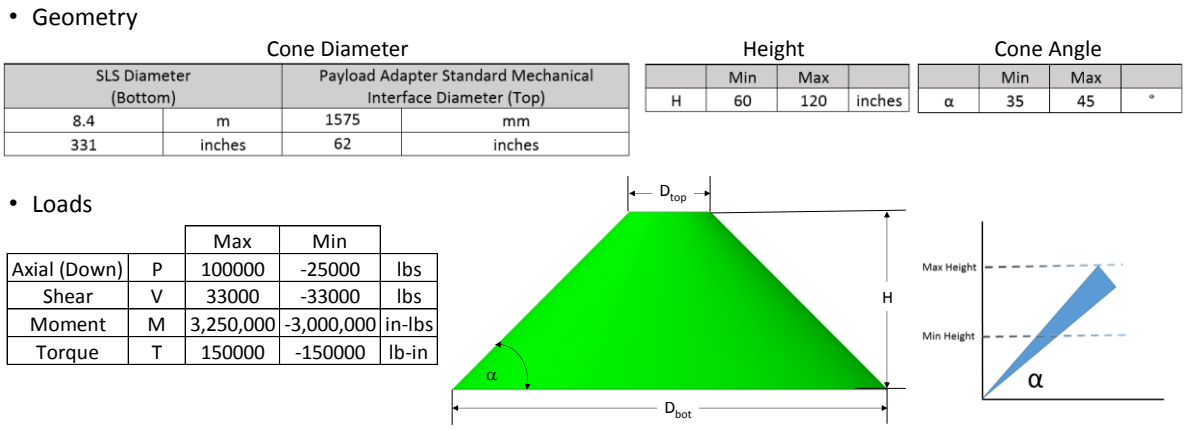

Figure 4 CTE Geometry and Loads.

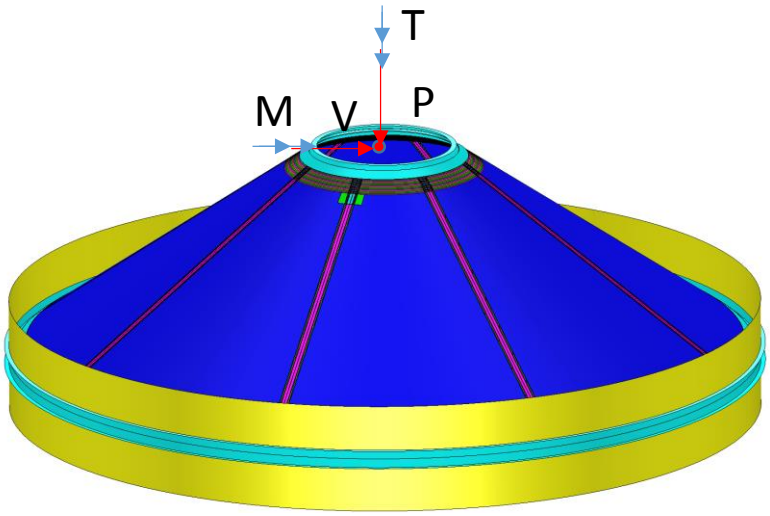

Figure 5 CTE FE Model Loads Model.

A finite element (FE) model was developed for several CTE cone angles and heights to determine the axial compressive line load for different CTE configurations. The axial compressive line load, N_x, from the analysis study is shown in Table 3. The 35° cone angle with the minimum top 62" diameter at the top of the cone gave the highest

compressive N_x line load. The N_x compressive line load for the CTE case with a 35-degree cone angle and a minimum 62" diameter is shown Figure 6. The CTE project decided to select this case (Case 4) since it had the highest line load and challenging joint geometries to establish the geometry of the *CTE Point Design*.

Table 3 N_x Compressive Line Load for CTE Angle and Height Configurations.

Case	Angle (deg)	Height (in)	Top Diameter (in)	Highest Nx (lb/in)
1	45	60.0	211	-359
2	35	60.0	159.62	-576
3	45	120.0	91.0	-1065
4	**35**	**94.2**	**62.0**	**-2291**

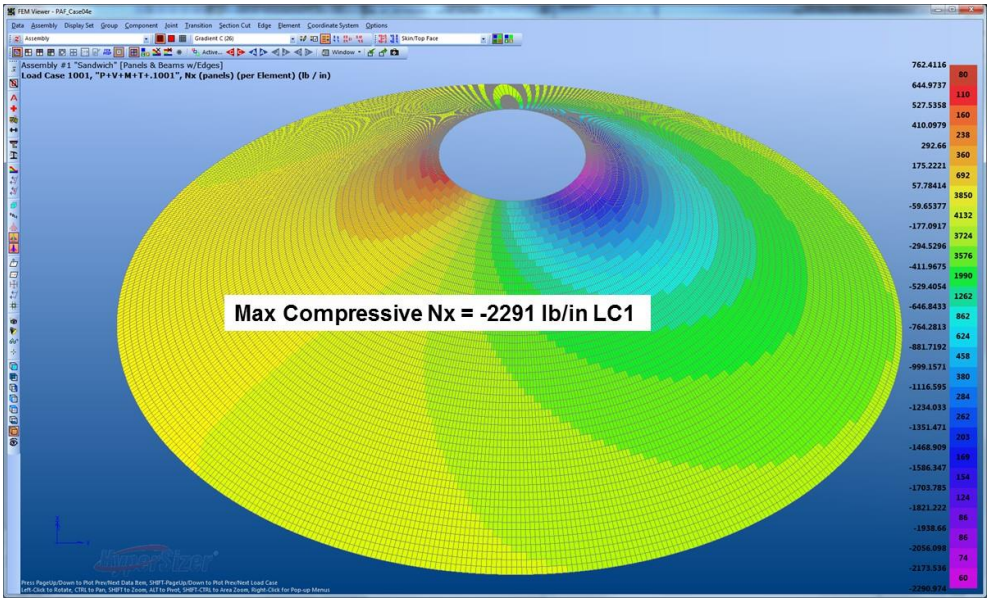

Figure 6 CTE FE Model Loads Model for 35 Degree Cone Angle with Minimum 62" Top Diameter.

B. CTE Longitudinal Bonded Joint Design, Sizing, and Analysis to Establish *CTE Point Design*

1. Global Analysis

A CTE FE global sizing and model was developed to size the *CTE Point Design*. Longitudinal joints were added to investigate the stiffness of the joints on the global buckling. The CTE global model is shown in Figure 7. From the bounding load conditions in Figure 4 a set of load cases were defined as shown in Table 4. Cases were made for the loads centered on a joint (100* load cases) and at the middle of the panel acreage with a 22.5 degree offset (200* load cases).

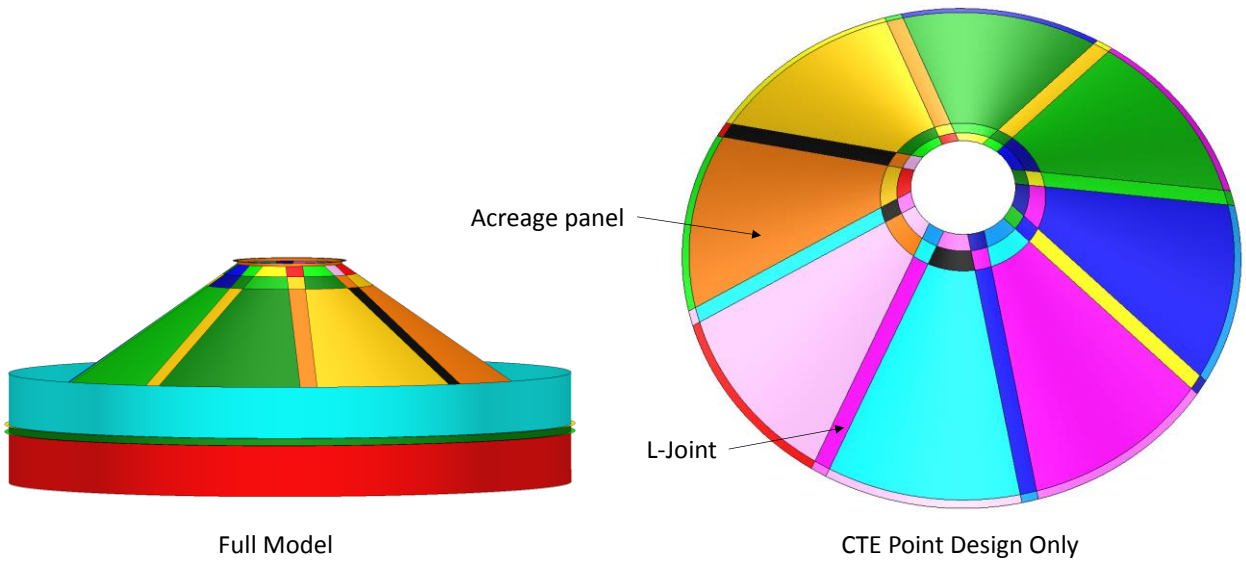

Figure 7 *CTE Point Design* Sizing Model.

Table 4 *CTE Point Design* Load Cases.

	Max	Min	
P	100000	-25000	lbs
V	33000	-33000	lbs
M	3,250,000	-3,000,000	in-lbs
T	150000	-150000	lb-in

0°	P	V	M	T	22.5°
1001	max	max	max	max	2001
1002	max	min	max	max	2002
1003	max	max	min	max	2003
1004	max	min	min	max	2004
1011	min	max	max	max	2011
1012	min	min	max	max	2012
1013	min	max	min	max	2013
1014	min	min	min	max	2014

HyperSizer [13] was used to size the *CTE Point Design* using the load cases in Table 4. The sizing called for the CTE sandwich panels to have a 1" Plascore 3.1 pcf 3/16-5056 honeycomb with 8-ply acreage facesheets of the IM7/8552-1 190 g/m^2 with a layup of [45/90/-45/0/0/-45/90/45] as shown in Figure 8 and Figure 9. This sized CTE conical structure was referred to as the *CTE Point Design*. An initial 6-ply sizing of the doublers for the longitudinal joints was assumed to provide the joint stiffness in the sizing analysis. The *CTE Point Design* line loads from the preliminary global analysis is shown in Figure 10. The line loads were then used in the preliminary longitudinal joint design discussed in the next section.

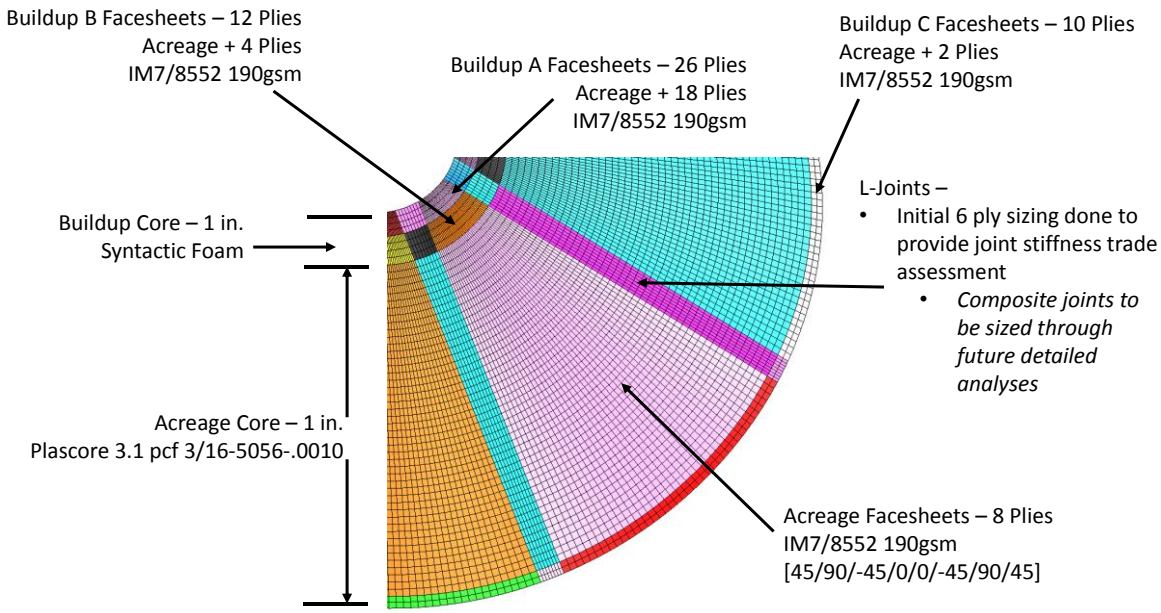

Figure 8 *CTE Point Design* Preliminary Sizing Details.

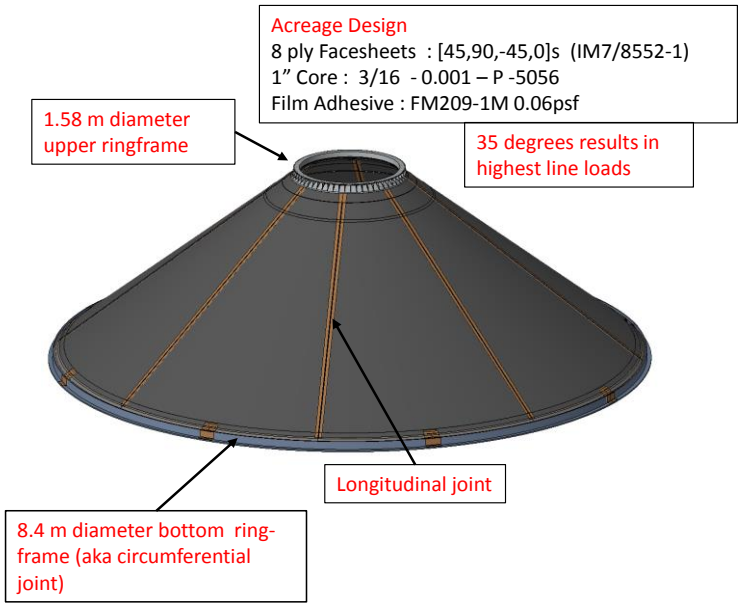

Figure 9 *CTE Point Design*.

	Acreage and Joints (Facesheets on joints have additional 6 ply doublers)								
	Max Nx			Max Ny			Max Nxy		
	LC 2001: Pmax, Vmax, Mmax, Tmax @ 22.5°			LC 1011: Pmin, Vmax, Mmax, Tmax @ 0.0°			LC 1002: Pmax, Vmin, Mmax, Tmax @ 0.0°		
	Nx	Ny	Nxy	Nx	Ny	Nxy	Nx	Ny	Nxy
Tension	301	533	497	1246	597	468	72	535	770
Compression	-1832	-577	-496	-863	-586	-499	-1540	-578	-758

	Acreage and Joints (Facesheets on joints set to the acreage properties)								
	Max Nx			Max Ny			Max Nxy		
	LC 1001: Pmax, Vmax, Mmax, Tmax @ 0.0°			LC 1001: Pmax, Vmax, Mmax, Tmax @ 0.0°			LC 1002: Pmax, Vmin, Mmax, Tmax @ 0.0°		
	Nx	Ny	Nxy	Nx	Ny	Nxy	Nx	Ny	Nxy
Tension	246	378	511	246	378	511	36	344	749
Compression	-1501	-484	-523	-1501	-484	-523	-1253	-450	-757

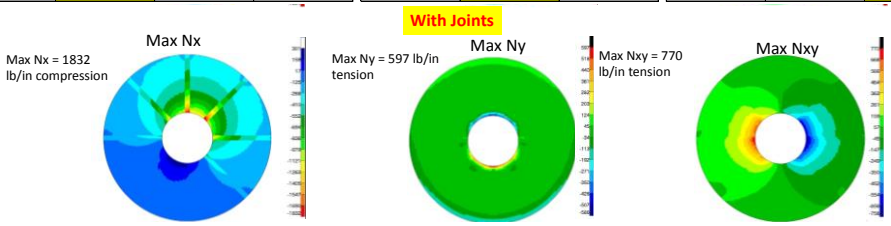

Figure 10 ***CTE Point Design*** **Preliminary Line Loads.**

2. Preliminary Joint Analysis

A preliminary longitudinal joint sizing was performed using the guidelines developed by the project. Using the *CTE Point Design* line loads in Figure 10 with a joint factor of safety of 2.0, a 6-ply joint doubler was determined using a project guidelines document which used the A4EI bonded joint software [14]. The width of the joint doubler was chosen to be 4.2 in. In addition, a bonded joint sizing tool available in HyperSizer called BondJo was also used to size the double lap joint, which resulted in a 5-ply doubler. For conservatism, the CTE project decided to proceed with a 6-ply composite fabric doubler in the bonded joint doubler. This was the starting point in the detailed global/local joint analysis discussed in the next section.

3. Detailed Joint Analysis

The objective of the detailed joint analyses was to predict the performance of the bonded doubler longitudinal joint while subjected to the CTE loads. A new global model with additional details based on the preliminary sizing results discussed in the last section was developed. A detailed local FEM using solid shell elements for the doubler and facesheet was also developed and is shown in Figure 11. The detailed local model used solid orthotropic elements to model the 1" Plascore honeycomb and adhesive which bonded the doubler to the facesheet. A portion of the global model was used in the local model as shown in Figure 12. The detailed local model was located at the top of the *CTE Point Design* centered on a joint. A picture showing the detailed local model overlaid on the global model is shown in Figure 13. In the local model the joint doubler originally was modeled as a 6-ply doubler based on the preliminary joint analysis sizing results, but later analyses showed that a 4-ply doubler was adequate for positive joint margins.

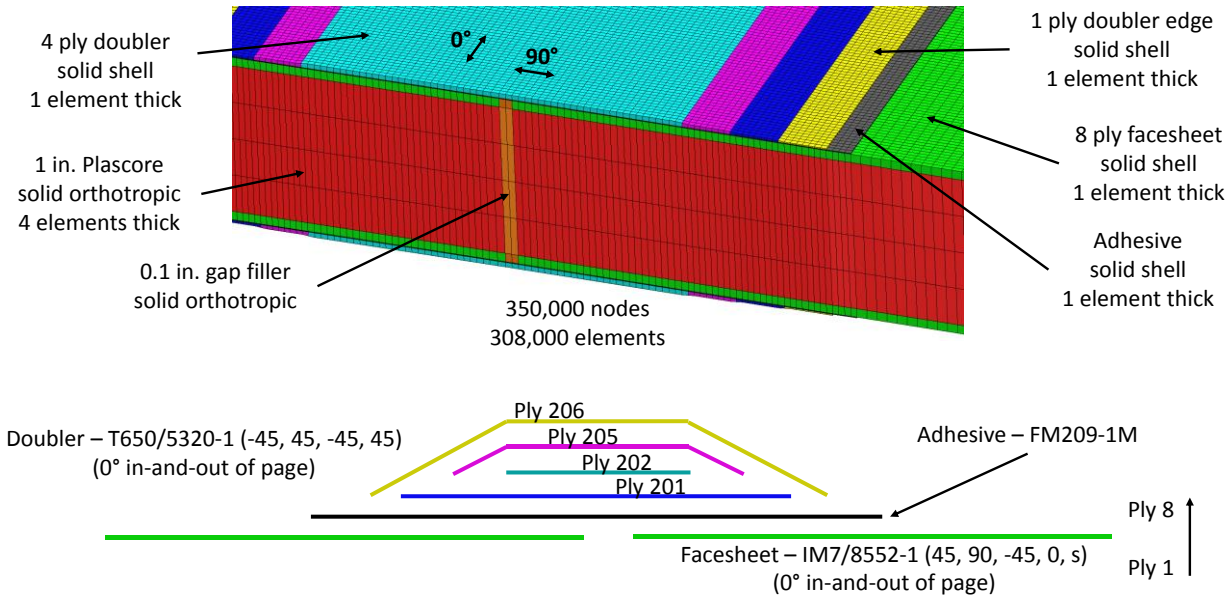

Figure 11 CTE Local Model with Joint Details.

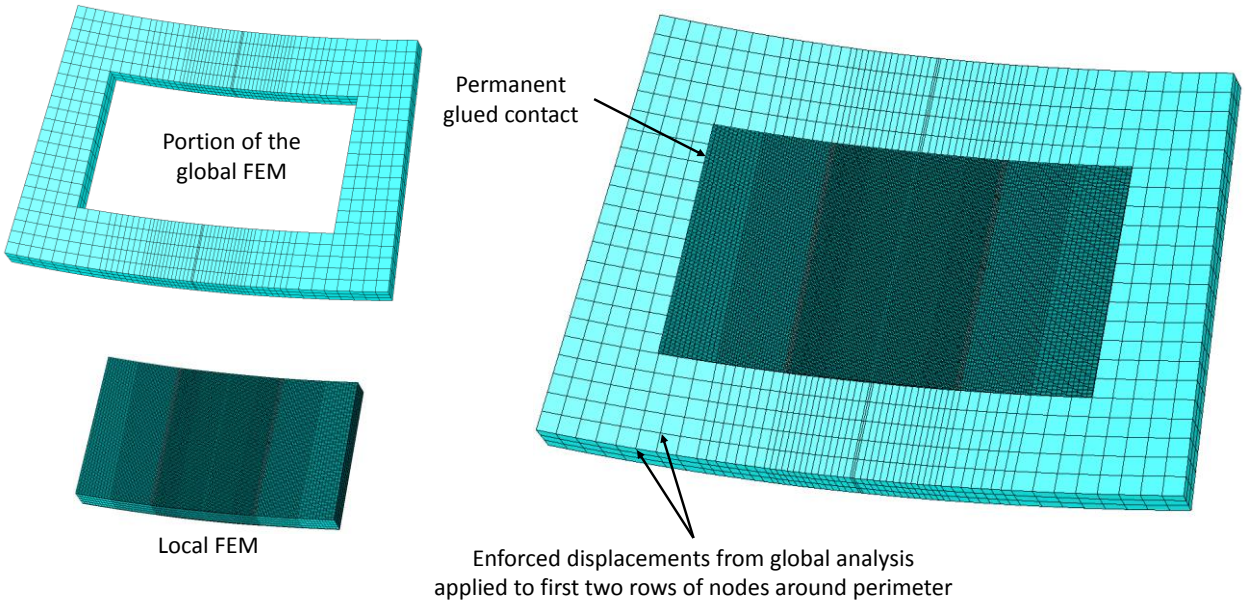

Figure 12 CTE Detailed Local Model.

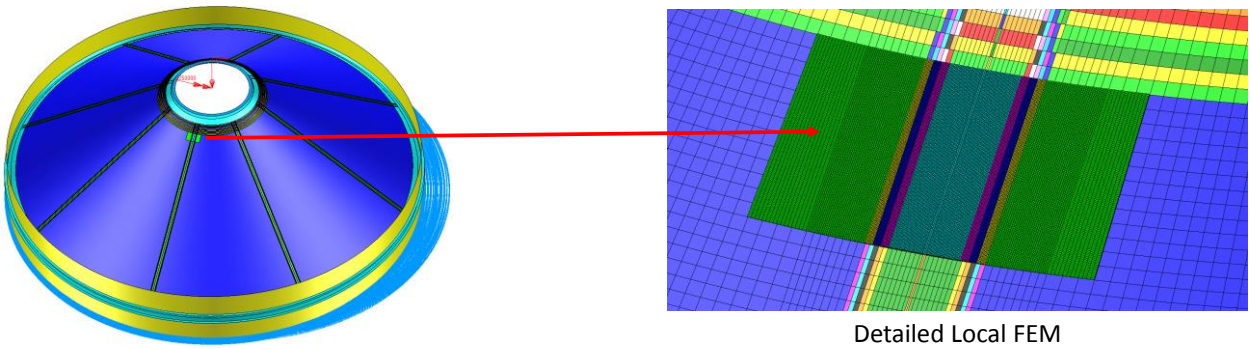

Figure 13 CTE Global-Local Model.

For the detailed local analysis using MSC Nastran [15], the global model was used to drive the local model. Displacements from the global model were applied as enforced displacements to the first outer two row of nodes around the perimeter of the local model. Multiple runs were analyzed based on the load cases in Table 4. Permanent glued contact was used to connect the coarse mesh of the local model to the fine mesh as shown in Figure 12. An illustration of the verification of the global-local analysis for the displacements is shown in Figure 14 with the detailed local displacement contour plot overlaid on the global model displacement contour plot.

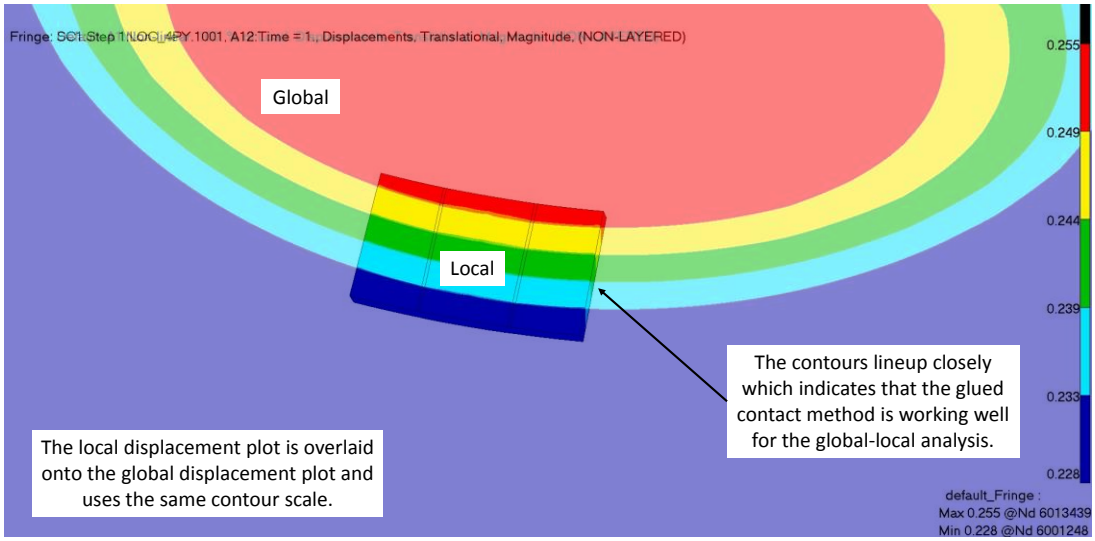

Figure 14 Verification of CTE Global-Local Model Analyses with Glued Contact.

The stresses at several rows of elements in the local model Figure 15 about 1 inch away from the glued contact boundaries were used to assess margins of safety for the composite bonded joint. The elements away from model boundaries were chosen in order to minimize the effects of boundary conditions on the stress results. The elements for the inner and outer facesheet, doubler, and adhesive elements were used to determine the margins of safety.

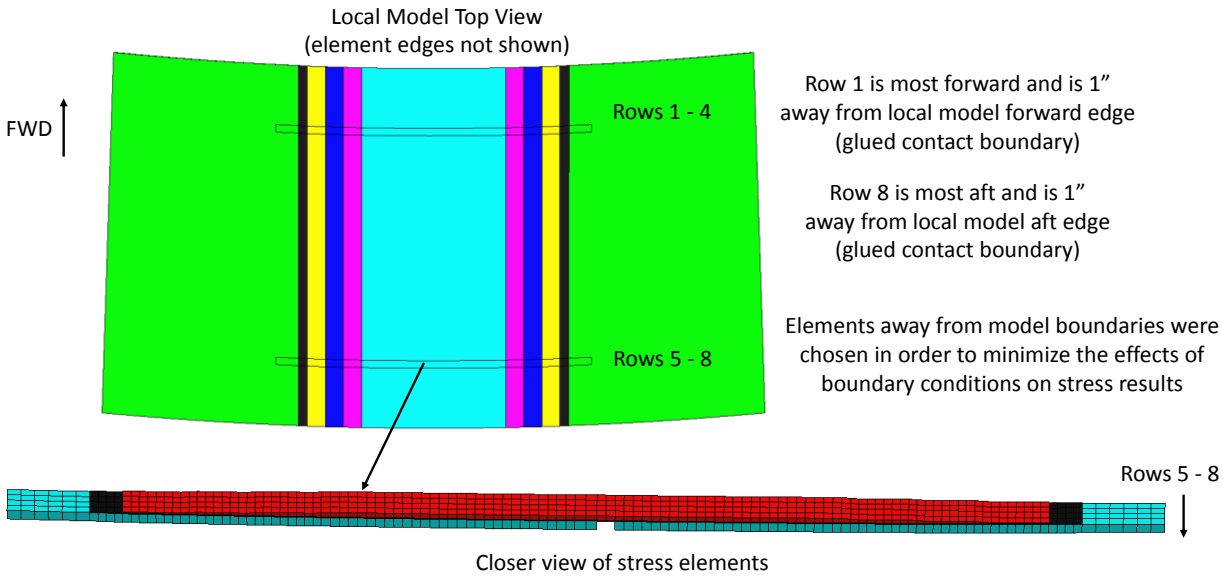

Figure 15 Local Stress Elements Used to Determine Joint Margins of Safety.

Various stress normal, shear, and transverse shear components were used to determine the joint margins of safety using the solid-shell facesheet and doubler elements. In addition, a failure criterion from Hoyt [16] listed in Equation 1 was used to assess the joint for delamination due to peel and transverse shear. The *Z* term refers to the through-the-thickness tensile strength of the composite adherends and the *R* term is the through-the-thickness shear strength of the laminate adherends. In additional normal, shear, and transverse shear stresses were used to check the adhesive for stress margins of safety. An additional failure criterion from Tong [17-18] consisting of peel, and longitudinal & transverse shear was also used as listed in Equation 2. The F_{peel} and F_{Shear} are the bondline peel and shear strengths.

$$\frac{\sigma_3}{Z}+\left(\frac{\tau_{13}}{R}\right)^2=1 \tag{1}$$

$$\left(\frac{\sigma_3}{F_{peel}}\right)^2+\left(\frac{\tau_{13}}{F_{shear}}\right)^2+\left(\frac{\tau_{23}}{F_{shear}}\right)^2=1,\ \ \sigma_3\geq 0$$

$$\left(\frac{\tau_{13}}{F_{shear}}\right)^2+\left(\frac{\tau_{23}}{F_{shear}}\right)^2=1,\ \ \sigma_3<0 \tag{2}$$

An iterative process was implemented to check the joint margins of safety for various doubler thicknesses. Originally, six plies in the doubler were used for the joint design. Ultimately, it was found that a 4-ply doubler was adequate for the joint design. All facesheet and doubler elements checked had positive margins of safety with a lowest margin of safety of +0.90. A linear model was used for the adhesive in the analysis which is conservative and the lowest margin of safety was +0.10 for one of the elements in the outer adhesive. After the final sizing iteration, the global model was updated and the joint line loads were again determined as shown in Figure 16. The details of the final CTE joint design is shown in Figure 17. The loads were then used to design and analyze the longitudinal joint sub-element test articles to assess the joint strength capability for the critical load cases for axial compression, hoop compression, and hoop tension.

	Max Panel **Axial**, **Nx** (lbs/in)		
	LC 1001: Pmax, Vmax, Mmax, Tmax @ 0.0°		
	Nx	Ny	Nxy
Tension	402	393	518
Compression	-1994	-490	-545

Max Panel **Hoop**, **Ny** (lbs/in)		
LC 1001: Pmax, Vmax, Mmax, Tmax @ 0.0°		
Nx	Ny	Nxy
402	393	518
-1994	-490	-545

Max Panel **Shear**, **Nxy** (lbs/in)		
LC 1002: Pmax, Vmin, Mmax, Tmax @ 0.0°		
Nx	Ny	Nxy
84	354	793
-1670	-450	-820

LC 1001 produced max Nx
Inline with local model

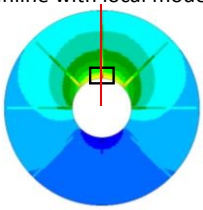

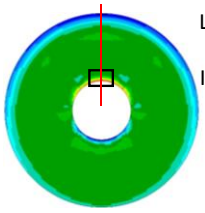

LC 1001 produced max compressive Ny
Inline with local model

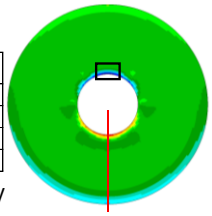

LC 1002 produced max Nxy
90° from local model

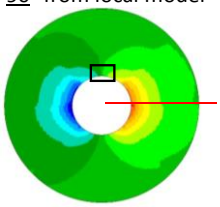

Max Panel **Hoop Tension**, **Ny**		
LC 1011: Pmax, Vmax, Mmax, Tmax @ 0.0°		
Nx	Ny	Nxy
1393	453	521
-1000	-429	-542

LC 1011 produced max tensile Ny
180° from local model

Loads Used in Global-Local Analysis

LC	Result
1001	Max Nx & Max Compressive Ny
1002	Max Nxy (Rotated 90°)
1011	Max Tensile Ny (Rotated 180°)

□ = Local Model

Figure 16 ***CTE Point Design*** **Final Line Loads.**

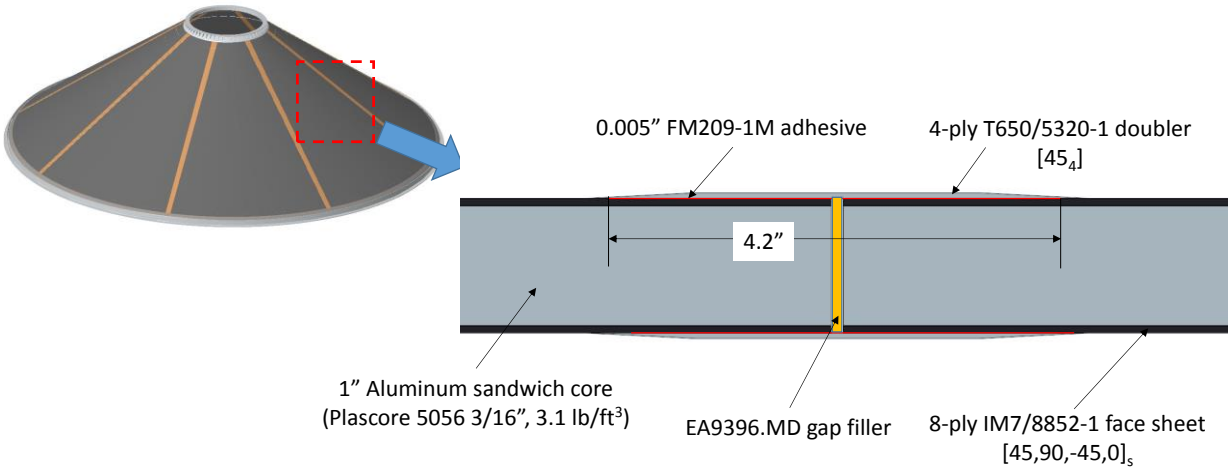

Figure 17 ***CTE Point Design*** **Joint Design.**

4. Global Buckling Analysis

The final analysis performed on the *CTE Point Design* with the final 4-ply doubler was a global buckling analysis. The buckling mode 1 is shown in Figure 18 with a global mode 1 buckling eigenvalue of 9.65. The required buckling mode 1 eigenvalue had to be larger than 4.0 based on a joint 2.0 FS with a SBKF of 0.50.

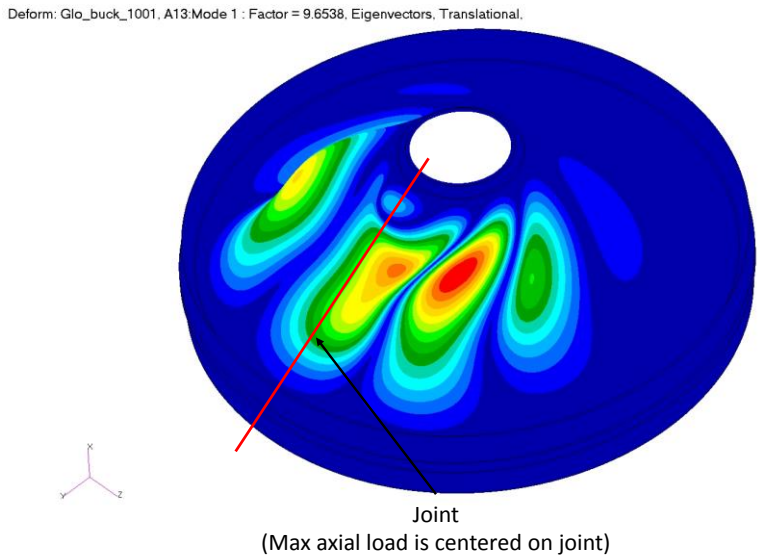

Mode 1
Buckling load factor = 9.65

Required buckling load factor
= 2.0/0.5 = 4.0
(Joint FS = 2.0, SBKF = 0.5)

This plot shows the first buckling mode shape. It is centered on the joint with the max displacement in the acreage to the side of the joint. This is because the joint is more stiff axially than the acreage.

Figure 18 *CTE Point Design* Buckling Mode 1 Shape.

C. CTE Longitudinal Joint Sub-Element Test Article Analysis and Design

A series of analyses and sensitivity studies were performed to size longitudinal joint sub-element test articles and to optimize the end conditions for the critical load cases for axial edge-wise compression, hoop edge-wise compression, and hoop edge-wise tension. The shear loading condition was determined to not be a critical load case by itself. The line loads from the final global model analysis shown in Figure 16 were used to design the test articles. The analyses were linear-elastic in nature and implemented to particularly investigate the top and bottom ends and their influence on the jointed panels stress state. The goal was to prevent premature failure by reducing the stress concentration at the coupons' ends/ corners and to preferably push the failure to the joint toward the middle of specimen, if possible. Further, in case of edge-wise compression coupons, the length of the test article had to be selected so that the failure is strength driven rather than buckling. The sections below describe the final design of the longitudinal joint sub-element test articles.

1. Axial Edge-Wise Compression (AEWC)

The AEWC coupons were sized to be 7.8" long by 6.2" wide as shown in Figure 19. The 7.8" long coupon provides sufficient length to ensure uniaxial loading in the specimen gage length while also being short enough that the first buckling mode critical load is beyond the load carrying capacity of the coupon with some reasonable margin (>30%). In preparation for testing, the load introduction ends of the bonded segments were designed to be potted in order to better stabilize the face-sheets and to prevent local crushing. The load introduction ends consisted of aluminum frames to contain the potting material and to provide additional lateral support during handling and testing. Edge relief was included by removing some of the potting material around the edges of the test article to alleviate high stress concentrations of the core. The goal was to design the AEWC sub-element coupons to fail at the joint location; however, multiple analysis iterations were unable to find a coupon design that would fail at the joint. Instead, the coupons were expected to fail at the load introduction ends of the coupons. The design limit load based on an axial compression line load of 1994 lb/in was 24.73 Kips with a 2.0 FS.

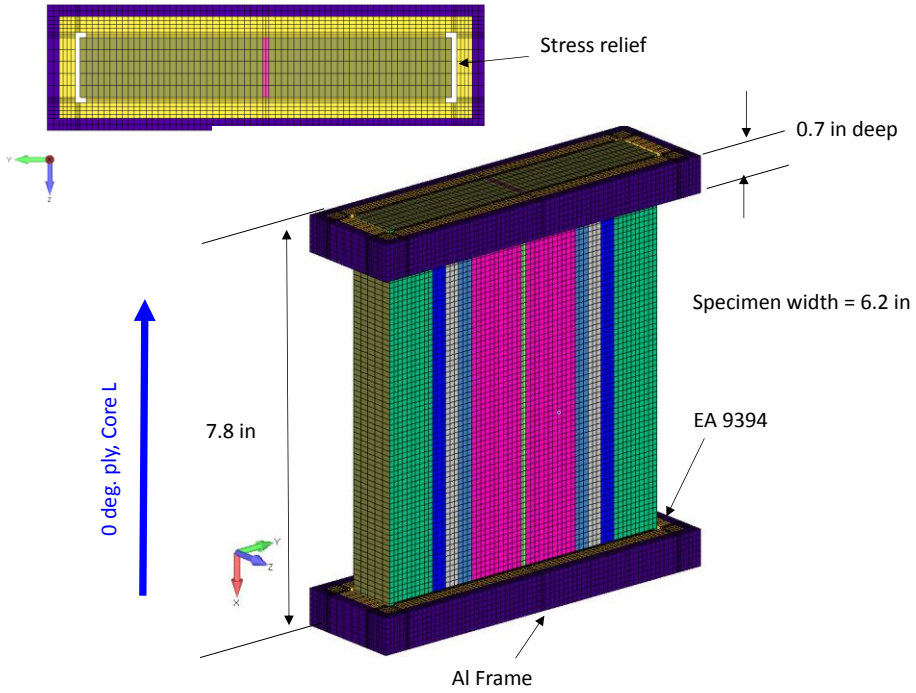

Figure 19 AEWC Coupon Size and Geometry (with Potted Ends).

2. Hoop Edge-Wise Compression (HEWC)

The HEWC sub-element coupons were the same size (7.8" long by 6.2" wide) as the AEWC sub-element coupons as shown in Figure 20. In preparation for testing, the load introduction ends of the bonded segments were designed to be potted in order to better stabilize the face-sheets and to prevent local crushing. The load introduction ends consisted of aluminum frames to contain the potting material and to provide additional lateral support during handling and testing. The HEWC coupons were designed to fail at the joint location according to preliminary analysis. The design limit load based on a hoop compression line load of 490 lb/in was 6.08 Kips with a 2.0 FS.

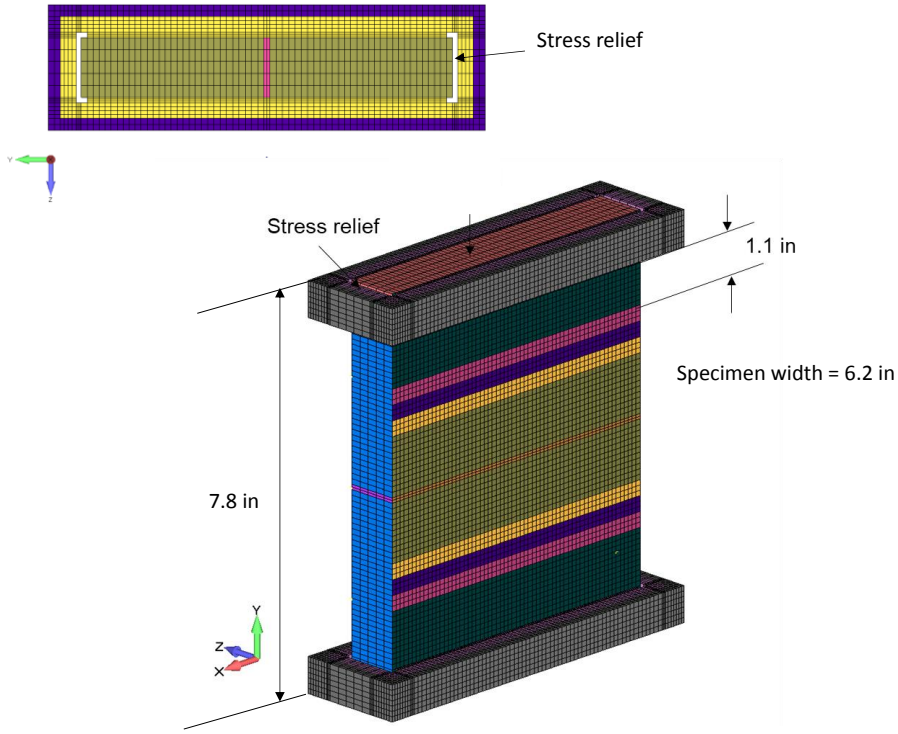

Figure 20 HEWC Coupon Size and Geometry (with Potted Ends).

3. Hoop Edge-Wise Tension (HEWT)

The HEWT test specimens were designed to have dimensions of 22" by 3" as shown in Figure 21. The maximum space between the grip faces in the test machine was 0.6 in.; hence, the hoop tension test specimen design was modified to fit within the grips. The core at the load introduction ends of the specimens was removed to a depth of 3.4 in. and an aluminum insert which was 1" thick at the core and tapered to 0.6" at the free end was inserted at either end of the panel and attached to the facesheet with adhesive. The test specimens were designed to fail at the joint location. The design limit load based on a hoop tension line load of 453 lb/in was 2.72 Kips with a 2.0 FS.

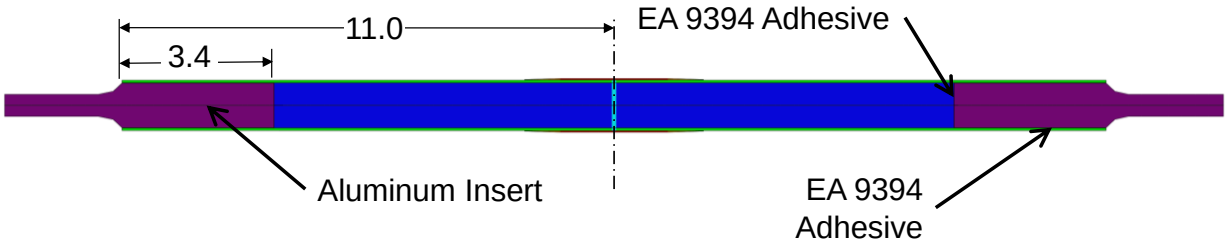

Figure 21 HEWT Coupon Size and Geometry (with Aluminum Inserts).

IV. Joint Manufacturing

Materials and manufacturing processes were chosen for the CTE project with the understanding that all facets must have the ability to scale-up for infusion into the SLS program. Longitudinal bonded joint assemblies for the development of joint test articles were manufactured in several phases, with portions of the manufacturing carried out at MSFC and LaRC. Acreage sandwich panels were manufactured at both MSFC and LaRC, while the longitudinal bonded joints themselves were fabricated at MSFC. Process specifications were developed for acreage sandwich panel manufacturing (primarily to ensure consistency in manufacturing operations at MSFC and LaRC) and longitudinal bonded joint fabrication (primarily to define, in detail, the surface preparation technique to be used). The following sub-sections detail manufacturing operations carried out for the longitudinal bonded joint assemblies considered herein.

A. Surface Preparation

In order to provide for flexibility in the down-selection of a surface preparation (abbreviated from this point forward as "surface prep") technique, options for surface prep were considered prior to the start of acreage sandwich panel manufacturing. This allowed for the consideration of techniques that alter the surface finish of the composite facesheets during manufacturing – namely, the use of peel plies. Peel plies are commonly used in composites manufacturing applications where bonding is to eventually occur; once the peel ply is removed immediately prior to bonding, the roughened, freshly fractured surface left behind provides for bonding primarily via mechanical interlock. The use of peel plies in surface prep inherently provides for consistency and repeatability, and also provides for some degree of surface protection in the period following manufacturing but prior to bonding (i.e. where incidental contamination could otherwise occur). Due to these considerations, a peel ply – specifically, 234 TFP (which was readily available at both MSFC and LaRC) – was selected for this study. 234 TFP is a thin woven fiberglass form, where the fibers themselves are coated with PTFE. Ultimately, a simple series of processes were used for surface prep in this study – immediately prior to bonding, the 234 TFP was removed and the newly exposed surfaces were flushed with reagent-grade isopropyl alcohol (IPA). The IPA was allowed to flash off, and the adhesive was applied. Due to the roughness imparted by the removal of the peel ply, the composite surfaces did not lend themselves to wiping. Each of the wipes preliminarily considered herein left behind visually observable amounts of residue (i.e. "lint") – thus the use of the IPA flush with no wiping.

In order to validate the selection of the aforementioned surface prep technique with the peel ply in terms of mechanical performance in an adhesive joint application, a series of single lap shear tests were carried out. While peak loads (and accordingly, single lap shear strengths) were recorded, the primary focus of these tests was to evaluate failure modes within the adhesive joint. Single lap shear parent panels were fabricated using the same surface prep technique (removal of 234 TFP followed by IPA flush) to be used on the longitudinal bonded joint assemblies. Single lap shear testing was carried out per ASTM D3165.

A total of 8 single lap shear specimens were tested. Table 5 shows results from this series of tests. Failure modes were quantified on the basis of relative area, where failure area percentages were calculated via digital image analysis. Most notable among the results shown in Table 5 is the fact that cohesive and substrate failure were observed to be the principal failure modes, and accordingly, adhesive failure was not observed to be prevalent. This signifies that the surface prep technique selected for this study (removal of 234 TFP followed by IPA flush) is suitable – it provides for a sufficiently strong adherend-adhesive interface, such that failure is forced away from said interface into either the bulk film adhesive or the composite laminate itself.

Table 5 Single lap Shear Test Results for Validation of Surface Preparation Technique.

Specimen	Peak Load (lb_f)	Single Lap Shear Strength (psi)	Failure (relative %)		
			Adhesive	Cohesive	Substrate
1	2115	4230	0	21	79
2	2234	4468	0	26	74
3	2108	4216	0	16	84
4	2147	4294	0	4	96
5	1976	3952	0	3	97
6	2255	4510	3	20	77
7	2160	4320	0	14	86
8	2223	4446	0	17	83
Mean	2152	4304	0	15	85
St. Dev.	90	180	1	8	8

B. Acreage Sandwich Panels

Following the selection and validation of the previously discussed surface prep technique, acreage sandwich panels were manufactured. A total of (30) 24"x48" sandwich panels were manufactured, with 15 panels fabricated at MSFC and 15 fabricated at LaRC. Facesheets were laid up in an 8-ply quasi-isotropic configuration ($[+45/90/-45/0]_s$) via automated fiber placement (AFP) using IM7/8552-1 prepreg slit tape (1/2" tows, 190 g/m^2. Sandwich panels were assembled using aluminum honeycomb core (3.1 pcf, 5056 alloy, 3/16" cells, 1" thick) and FM209-1M film adhesive (0.06 psf). Core ribbon direction and 0° fiber direction were oriented in the same direction. Following facesheet layup and sandwich panel assembly, sandwich panels were co-cured – that is, facesheets were cured and bonded to the core in the same operation in an autoclave. Following the cure, acreage sandwich panels were inspected via infrared thermography with the peel ply still on the surface. The CTE project developed a standardized NDE process for characterizing potential acreage sandwich panel defects.

C. Longitudinal Bonded Joints

Following acreage sandwich panel manufacturing, longitudinal bonded joint assemblies were fabricated. Acreage sandwich panels were sectioned (so as to accommodate eventual bonded joint test specimens), and said sections were affixed adjacent to one another with a 0.10" gap between them. Panel-to-panel gaps were then filled with EA9396.6MD, which is a room temperature curing filled epoxy. Following gap filler injection and cure, the 234 TFP peel ply was removed from the acreage sandwich panels and the surfaces were flushed with IPA. Composite doublers were then laid up and placed in a double strap configuration across the panel-to-panel junctions. Doublers were laid up with T650/5320-1 out-of-autoclave prepreg fabric (3k tows, plain weave) in a $[+45]_4$ configuration. FM209-1M film adhesive (0.06 psf) was used between the cured acreage sandwich panels and the uncured composite doublers. Figure 22 shows the longitudinal bonded joint manufacturing process in detail.

Both the film adhesive and the doublers were cured and bonded to the acreage sandwich panels in a single operation (i.e. a "co-bond" process) in an oven. An oven cure was used for the doubler bonding process to reduce process variability for an accelerated CTE project schedule. Following the cure, longitudinal bonded joint assemblies were inspected via infrared thermography. A NDE joint standard was developed for the inspection for porosity and bondline defects.

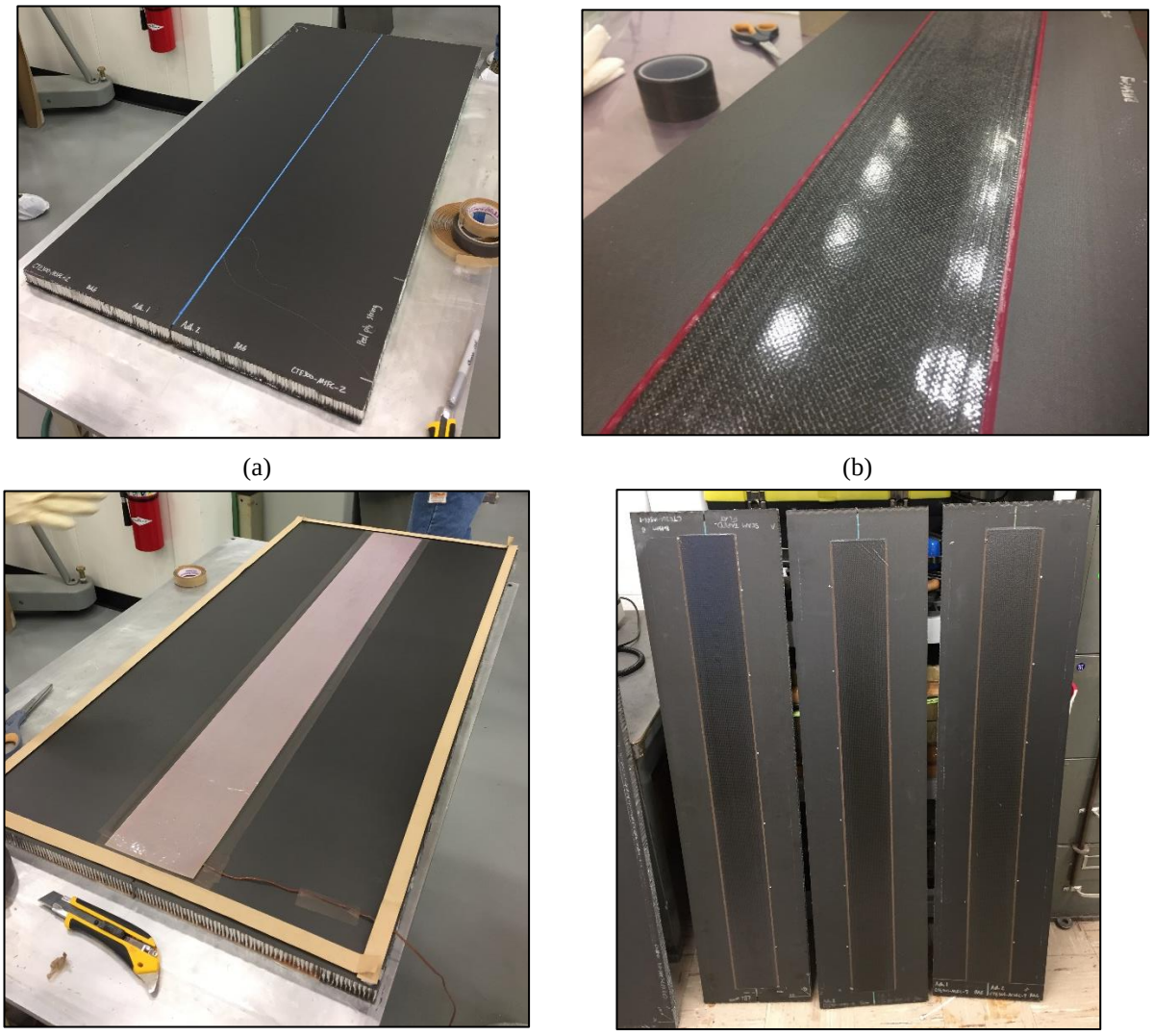

Figure 22 Longitudinal Bonded Joint Manufacturing: (a) acreage sandwich panel sections following gap filler injection, (b) composite doubler following layup, (c) preparation for oven cure, and (d) series of completed longitudinal bonded joint assemblies.

D. Longitudinal Joint Sub-Element Test Article Fabrication

After the longitudinal bonded joint panels were manufactured at MSFC, the panels were sent to GSFC for fabrication into longitudinal jointed sub-element test articles. For the planned testing, 17 AEWC sub-element test coupons, 13 HEWC sub-element test coupons, and 19 HEWT sub-element test coupons were fabricated and sent to Southern Research in Birmingham, AL for testing.

V. Longitudinal Joint Sub-Element Testing

In order to assess the structural performance of the CTE longitudinal composite sandwich bonded joint design and to validate the structural models for joint failure prediction, the CTE team devised an extensive test matrix determined by the structural analysis effort for various critical loading conditions based on the longitudinal joint. These loading conditions included axial compression, hoop compression, and hoop tension applied loadings. Multiple replicates of sub-element jointed test articles were machined from the composite sandwich bonded jointed panels and tested for failure both in pristine conditions and with 6 ft-lbs of impact-damage at the center of the joint at Southern Research. The energy level of the impact damage was chosen based on impact survey testing on CTE bonded joint samples to understand the effects of various energy levels to obtain barely visible impact damage (BVID). This section includes a summary of the test results for the AEWC, HEWC, and HEWT joint sub-element coupon testing conducted at SR from May-July 2018. Additional details of the test results and analysis correlation are expected in future papers.

1. Axial Edge-Wise Compression (AEWC)

The test stand & compression test setup for both pristine and impacted AEWC coupons is shown in Figure 23. The coupon is placed between a flat square platen at the bottom and a thick rectangular steel block, covering the entire width and thickness of the coupon, on the top. Above the thick steel block, a circular cross-section steel block is placed. The load capacity of the test stand is 60 Kips. The AEWC sub-element coupons were instrumented with strain gages and a digital image correlation (DIC) system to obtain full field, displacement and strain contours.

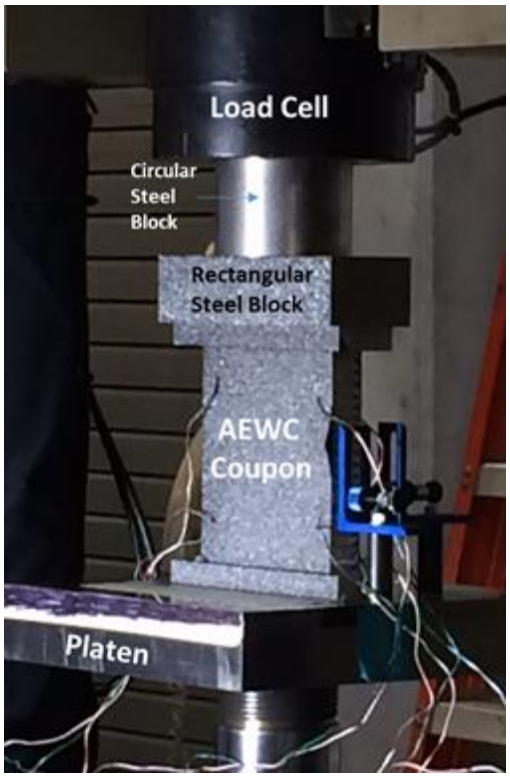

Figure 23 Test Setup & Strain Gauge Configuration of AEWC Coupon.

a) Pristine Coupons

Table 6 reports the failure mode and the failure load of all 10 pristine coupons along with the axial strain at the center of the joint just before the failure load. One of the coupons had an initial geometric imperfection in the form of a dent on one side noticed in initial inspection of the coupons, which caused it to fail at a lower load than others and hence was excluded in evaluating the average failure load. The failure modes 1 & 2 represent fiber failure in facesheet at grips and delamination between facesheet plies respectively. The average failure load for all AEWC pristine coupons was 40.45 Kips which was significantly higher than the coupon design load of 24.73 Kips with a 2.0 FS based on the line loads from the updated global finite element model. Pre-test analysis failure predictions of the AEWC coupons were within 8.8% of the average test failure load. Post-test analysis failure predictions improved to 3.3% based on updates in the material properties and including the nonlinear behavior of the FM209-1M film adhesive and potting material.

Table 6 Test Data of AEWC Coupons.

AEWC COUPON ID	Test Failure Load (kips)	Axial Strain SG-9 (microns)	Failure Mode
CTE-301-3-AEWC - 1	40.438	6995	1 & 2
CTE-301-3-AEWC – 2*	35.178*	-	1 & 2
CTE-301-3-AEWC - 3	42.283	7932	1
CTE-301-3-AEWC - 4	38.592	7287	
CTE-301-3-AEWC - 5	39.987	7170	1
CTE-301-4-AEWC - 1	38.789	7016	1
CTE-301-4-AEWC - 2	42.292	7410	1
CTE-301-4-AEWC - 3	40.422	7594	1
CTE-301-4-AEWC - 4	40.708	7475	1
CTE-301-4-AEWC - 5	40.555	7368	1
Average	**40.452**	**7360.88**	

In Figure 24 typical failure modes of AEWC coupons are presented. Final joint failure due to fiber damage in the facesheet at the grips was present in all of the coupons. Secondary damage such as delamination occurred during the energy dissipation process.

Figure 24 Typical Damage Modes in AEWC Coupons.

b) Impact-Damaged Coupons

Seven impacted AEWC coupons were tested under compressive load. The impact location on the coupon is presented in Figure 25. Failure loads and failure modes of each coupons are presented in Table 7. Failure mode 1 indicates fiber damage in facesheet and failure mode 2 indicates delamination at the facesheet ply interfaces. The average failure load of the impacted AEWC coupons is 32.35 Kips which is about 20% less than the pristine coupons. However, the average failure load was still higher than the coupon design load of 24.73 Kips with a 2.0 FS. Typical damage and failure modes of an impacted AEWC coupon are presented in Figure 26. Significant delaminations were noticed in all but one coupon. Analysis failure predictions were not performed for the impact-damaged AEWC coupons.

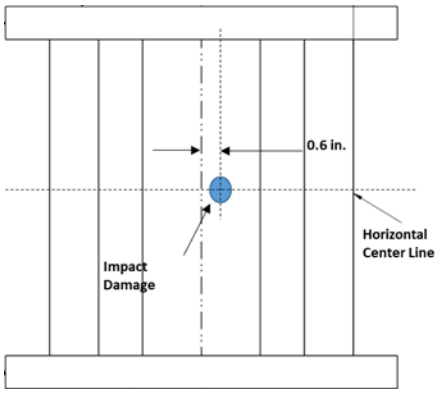

Figure 25 AEWC Coupon Impact Damage Location.

Table 7 Failure Load & Mode of Impacted AEWC Coupons.

AEWC COUPON ID	Max Test Failure Load (kips)	Failure Mode
CTE-301-7-AEWC –D- 1	33.231	1 & 2
CTE-301-7-AEWC –D- 2	30.481	2
CTE-301-8-AEWC - 1	32.119	
CTE-301-8-AEWC - 2	30.298	
CTE-301-8-AEWC - 3	33.790	1 & 2
CTE-301-8-AEWC - 4	33.741	1 & 2
CTE-301-8-AEWC - 5	32.757	1
Average	**32.345**	

Figure 26 Failure Modes of Impacted AEWC Coupons.

2. Hoop Edge-Wise Compression (HEWC)

The test stand and compression test setup for both pristine and impacted HEWC coupons is the same as in the AEWC test shown previously in Figure 23. The coupon is placed between a flat square platen at the bottom, and a thick rectangular steel block, covering the entire width and thickness of the coupon, on the top. A circular cross-section steel block is placed above the thick steel block. The load capacity of the test stand is 60 Kips.

a) Pristine Coupons

Table 8 reports the failure modes and failure load of all 7 coupons along with the axial strain at center of the joint just before the failure load. Two coupons had their center strain gauge fail before the final failure of the coupons and hence were not considered for averaging. The failure modes "1" and "2" represent delamination between facesheet plies and fiber failure in the outer facesheet ply, respectively. The average failure load for all HEWC pristine coupons was 21.42 Kips which was significantly higher than the coupon design load of 6.08 Kips with a 2.0 FS. Typical failure modes of the HEWC coupons are presented in Figure 27. The dominant failure mode of the joint in all of the coupons was the delamination damage between the facesheet plies. The delamination damage leads to fiber failure in the outer ply of the facesheet laminate in some coupons. Pre-test analysis failure predictions of the HEWC coupons were within 3% of the average test failure load. Post-test analysis failure predictions were not needed since the pre-test predictions were within 5% of the test data which was a goal of the project.

Table 8 Test Data of HEWC Coupons.

HEWC COUPON ID	Test Failure Load (kips)	Axial Strain SG-9 (microns)	Failure Mode	Comment
CTE-301-5-HEWC - 1	22.02	6592	1 & 2	
CTE-301-5-HEWC - 2	22.75	6495	1	
CTE-301-5-HEWC – 3*	20.44	3058*	1	*Max Strain reached at 11.75 Kips
CTE-301-9-HEWC - 1	21.75	6188	1	
CTE-301-9-HEWC - 2	22.30	6562	1	
CTE-301-10-HEWC - 1	20.04	6348	1	
CTE-301-10-HEWC – 2*	20.67	5098*	1	*Max Strain reached at 17.64 Kips
Average	**21.42**	**6437**		

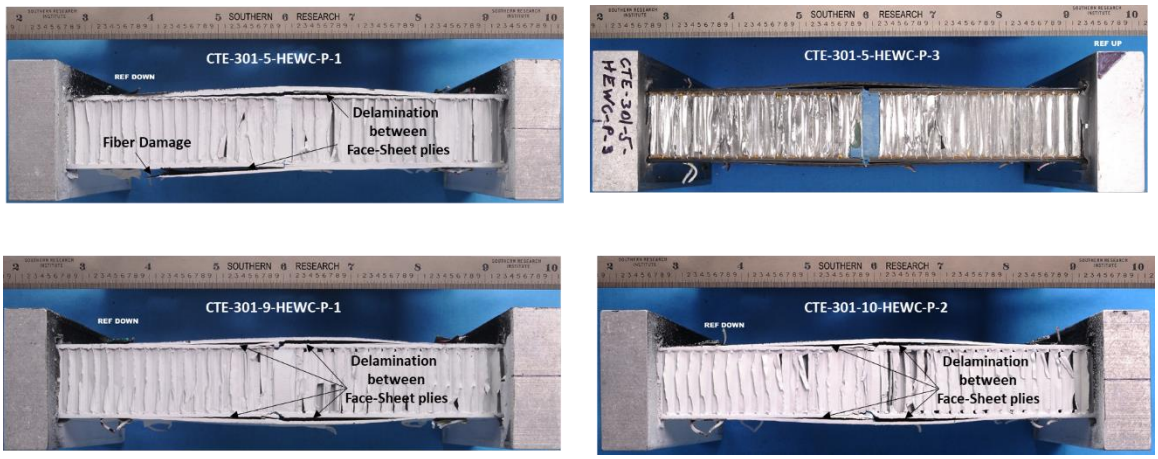

Figure 27 Typical Damage Modes in HEWC Coupons.

b) Impact-Damaged Coupons

Six impact-damaged HEWC coupons were tested under compressive load. The impact location on the coupon is presented in Figure 28. Failure loads and failure modes of each coupons are presented in Table 9. Failure mode "1" indicates delamination between facesheet plies and failure mode "2" indicates fiber failure in outer facesheet ply. The average failure load of impacted HEWC coupons is 20.42 Kips which is 4.6 % less than the pristine coupons. The average test failure load was still significantly higher than the coupon design load of 6.08 Kips with a 2.0 FS. Typical damage and failure modes of the impacted HEWC coupons are presented in Figure 29. Significant delaminations were noticed in all of them. Analysis failure predictions were not performed for the impact-damaged HEWC coupons.

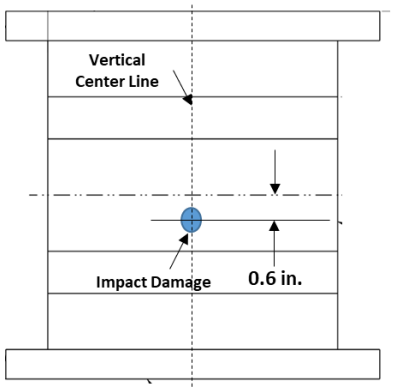

Figure 28 HEWC Impact Damage Location.

Table 9 Failure Load & mode of Impacted HEWC Coupons.

AEWC COUPON ID	Max Test Failure Load (kips)	Failure Mode
CTE-301-6-HEWC-D- 1	21.63	1
CTE-301-6-HEWC-D- 2	22.96	1
CTE-301-7-HEWC-D-1	20.88	1
CTE-301-7-HEWC-D-2	19.01	1
CTE-301-7-HEWC-D-3	19.54	1
CTE-301-7-HEWC-D-4	18.51	1 & 2
Average	**20.42**	

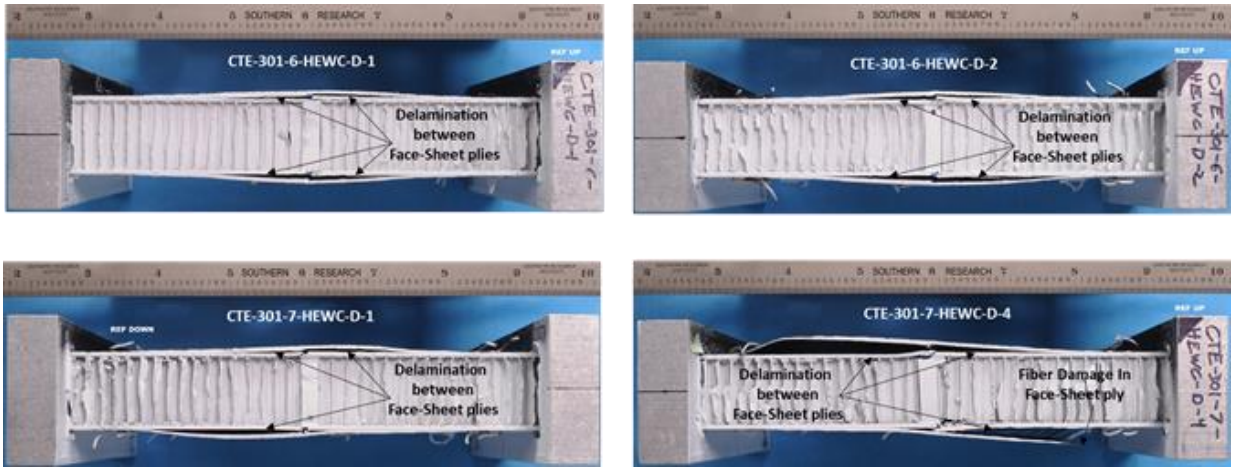

Figure 29 Typical Damage Modes of Impacted HEWC Coupons.

3. Hoop Edge-Wise Tension (HEWT)

The test stand for the HEWT coupon tests at Southern Research is shown in Figure 30. The sub-element coupons were gripped in the test machine and pulled under tension loading until failure.

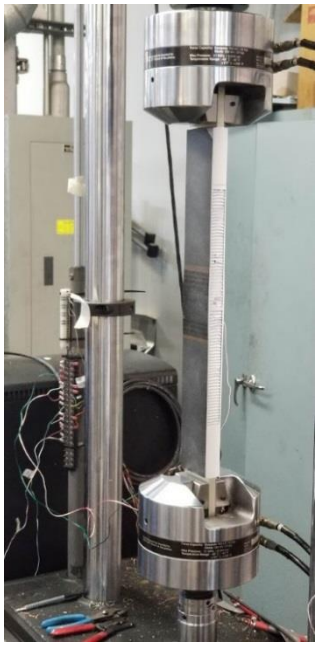

Figure 30 Test Set-up for HEWT Test at Southern Research.

a) Pristine Coupons

Ten HEWT sub-element coupons were tested under a tensile load. Table 10 reports the failure modes and failure load of all the 10 HEWT coupons along with the axial strain at center of the joint before failure. The failure modes of the tested coupons were "Delam" (delamination between facesheet plies) and NSF (net-section failure of doubler plate). Four of the coupons failed due to "Delam" on one side and NSF on the other side. Four of the coupons failed due to NSF on both sides and two of the coupons failed due to "Delam" on both sides. The average failure load of the joint in tension, is 15.01. Kips which was significantly higher than the coupon design load of 2.72 Kips with a 2.0 FS. Figure 31 presents typical failure modes of the HEWT coupons. A large scatter in failure mode data was noticed for this joint. Predominant failure modes of the joint are "Delam" and "NSF". Pre-test analysis failure predictions of the HEWT coupons were within 1% of the average test failure load. Post-test analysis failure predictions were not needed since the pre-test predictions were within 5% of the test data which was a goal of the project. Further details of the analysis are discussed in reference 19.

Table 10 Test Data of HEWT Coupons.

Coupon ID	Test Failure Load (kips)	Strain at failure (SG-1), Micron	Failure Mode
CTE-300-1-HT-P-1	16.117	0.02	Delam/NSF
CTE-300-1-HT-P-2	13.767	0.014	Delam/NSF
CTE-300-1-HT-P-3	15.584	0.0197	Delam/NSF
CTE-300-1-HT-P-4	13.003	0.0138	Delam
CTE-300-1-HT-P-5	13.897	0.015	Delam
CTE-300-3-HT-P-1	15.666	0.026	NSF
CTE-300-3-HT-P-2*	15.196	0.027	NSF
CTE-300-3-HT-P-3	15.018	0.022	Delam/NSF
CTE-300-3-HT-P-4	15.891	0.035	NSF
CTE-300-3-HT-P-5	16.000	0.029	NSF
Average	**15.014**		

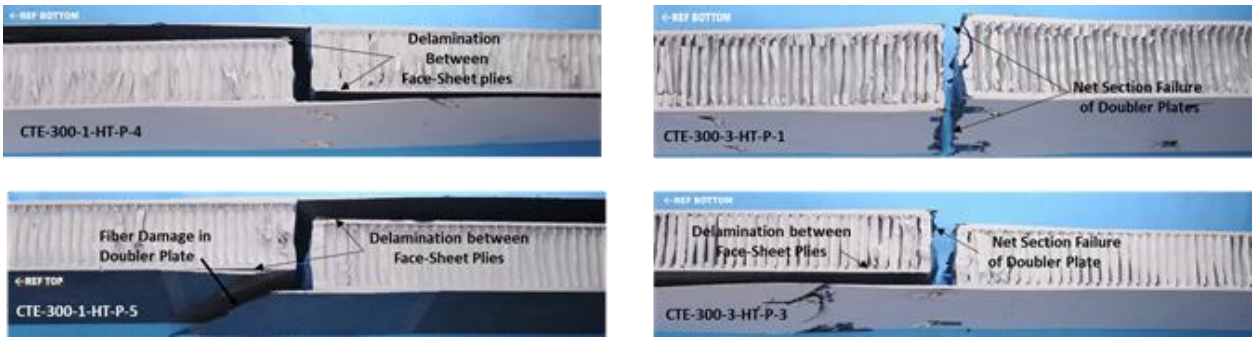

Figure 31 Typical Damage Modes in HEWT coupons.

b) Impact-Damaged Coupons

Nine impact damaged HEWT coupons were tested under tensile load. The impact location on the coupon is presented in Figure 32. Failure loads and failure modes of each coupons are presented in Table 11. Failure mode of "Delam" indicates delamination between facesheet plies and failure mode of "NSF" indicates net section failure of doubler plate/plates. The average failure load of impacted HEWT coupons is 15.29 Kips which is 1.8 % more than the pristine HEWT coupons. The design load of the coupons was 2.72 Kips with a 2.0 FS. Five coupons failed due to a combination of "Delam" and "NSF," and three coupons failed due to "NSF" in one of the doubler plates, and one coupon did not have a photograph to determine the mode of failure. Typical damage and failure modes of the impact-damaged HEWT coupons are presented in Figure 33. Significant delaminations were noticed in all of them.

Table 11 Failure Load & Mode of Impacted HEWT Coupons.

Coupon ID	Test Failure Load (kips)	Strain at failure (SG-1), Micron	Failure Mode
CTE-300-1-HT-D-1	11.927	0.0136	NSF (1 Doubler plate)
CTE-300-1-HT-D-2	15.636	0.0237	Delam/NSF
CTE-300-1-HT-D-3	14.637	0.0198	Delam/NSF
CTE-300-1-HT-D-4	15.627	0.0226	Delam/NSF
CTE-300-3-HT-D-1	11.067	0.011	NSF (1 Doubler plate)
CTE-300-3-HT-D-2	14.986	0.018	
CTE-300-3-HT-D-3	15.28	0.0182	Delam/NSF
CTE-300-3-HT-D-4	15.598	0.0287	NSF
CTE-300-3-HT-D-5	15.237	0.0213	Delam/NSF
Average	**15.286**		

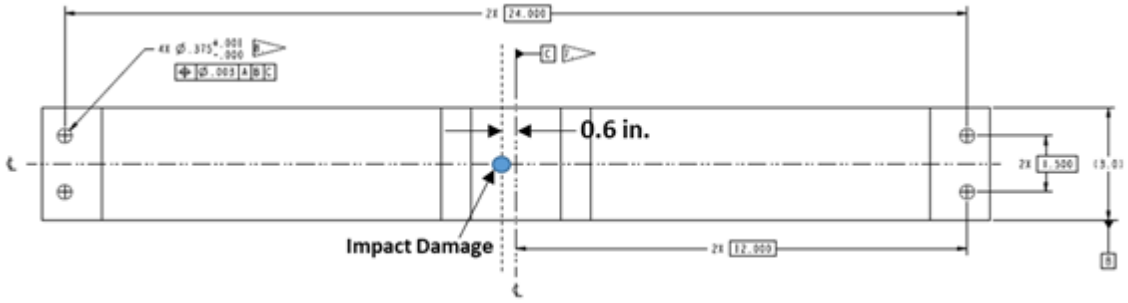

Figure 32 HEWT Impact Damage Location.

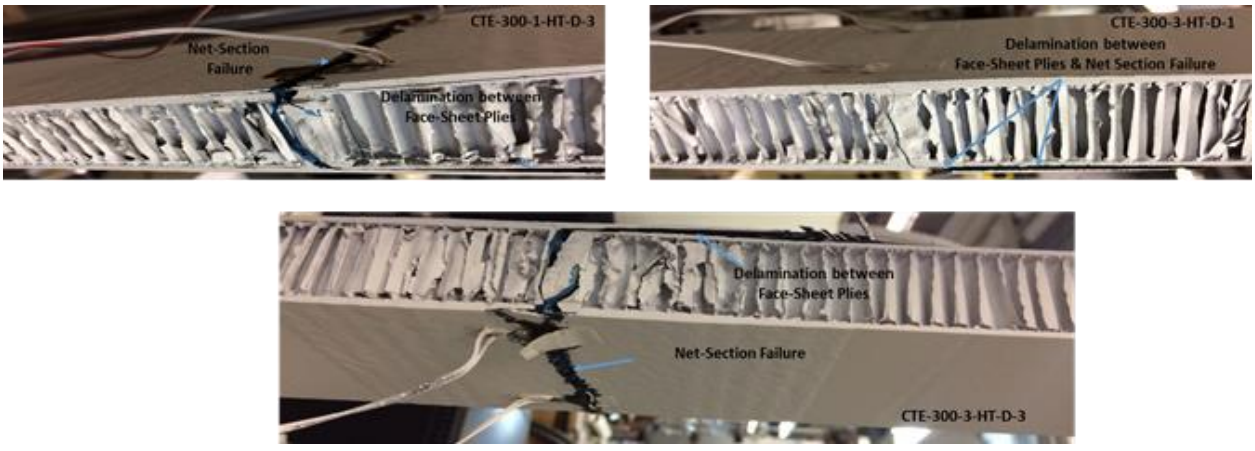

Figure 33 Typical Damage Modes in Impact-Damaged HEWT Coupons.

VI. Concluding Remarks

The NASA Composite Technology for Exploration (CTE) Project is developing and demonstrating critical composite technologies with a focus on composite bonded joints; incorporating materials, design/analysis, manufacturing, and tests that utilize NASA expertise and capabilities. The project has goals of advancing composite technologies providing lightweight structures to support future NASA exploration missions. In particular, the CTE project will demonstrate weight-saving, performance-enhancing composite bonded joint technology for Space Launch System (SLS)-scale composite hardware. Advancements from the CTE project may be incorporated as future block upgrades for SLS structural components.

This paper discussed the details of the development including materials, design & analysis, manufacturing of a composite sandwich bonded longitudinal joint for a generic space launch vehicle structure called the *CTE Point Design.* The *CTE Point Design* is a conical sandwich structure with a 35-degree angle consisting of eight composite sandwich segments joined together with a double lap composite joint. The segmented panels are a sandwich construction with 3.1-lb/ft^3, 1-in. thick perforated Plascore aluminum core (5056) with (3/16-in.) hexagonal cells and 8-ply quasi-isotropic IM7/88552-1 facesheets with a layup of $[45/90/-45/0]_S$. The material for the doubler plates is a T650/5320-1 epoxy and carbon fiber woven prepreg fabric with a layup of $[45_4]$. Doubler plates were bonded to the sandwich panels with FM209-1M adhesive. The doubler plates were 4.2-inches wide. During the joining process, an adhesive paste (EA 9396 6MD) was injected to fill a 0.1-in. gap between the two panel segments. Longitudinal bonded joint sub-element test articles were fabricated and tested for several loading conditions to test the capability of the joint design for the as designed loads. The test results show that test failure loads for the composite longitudinal bonded joint design significantly exceeds the joint design loads with a 2.0 factor of safety for both pristine and impact-damage coupons. The analysis pre-test failure predictions for all sub-element bonded joint test coupons were all within 10% of the average test coupon failure load. This testing and analysis provides confidence in the potential use of composite bonded joints for future launch vehicle structures.

Acknowledgments

This work was conducted as part of the Composite Technology for Exploration Project funded by the Space Technology and Mission Directorate (STMD) Game Changing Development (GCD) Program and the Space Launch System (SLS) Program.

References

[1]Kirsch, Michael, T. "Composite Crew Module: Primary Structure," NASA/TM-2011-217185.

[2]Johnson, T. F., Sleight, D. W., and Martin, R. A., "Structures and Design Phase I Summary for the NASA Composite Cryotank Technology Demonstration Project," 54th AIAA/ASME/ASCE/AHS/ ASC Structures, Structural Dynamics, and Materials Conference, Boston, MA, April 2013.

[3]Fikes, J. C., Jackson, J. R., Richardson, S. W., Thomas, A. S., and, T. O., and Miller, S. G., "Composites for Exploration Upper Stage," NASA/TM-2016-219433, December 2016.

[4]Sleight, David. W., Rosario, S., Johnson, T. F., and Shular, D. A., "Composite Cryotank Technology Demonstration 5.5-Meter Diameter Pre-Test, Analysis and Test Readiness," NASA/TM-2016-219325.

[5]Mann, T., Smeltzer, S., Grenoble, R. W., Mason, B. H., Rosario, S., & Fairbairn, R., "Sizing and Lifecycle Cost Analysis of an Ares V Composite Interstage", AIAA 2012-1770, 53rd AIAA/ASME/ASCE/AHS/ASC Structures, Structural Dynamics, and Materials Conference, Honolulu, HI, April 2012.

[6]Hexcel 8552 IM7 Unidirectional Prepreg 190 gsm & 35%RC Qualification Material Property Data Report, NCAMP Test Reports#: CAM-RP-2009-015 Rev A, April 22, 2011.

[7]Hexcel 8552 IM7 Unidirectional Prepreg 190 gsm & 35%RC Qualification Statistical Analysis Report, NCAMP Report#: NCP-RP-2009-028 Rev N/C, June 21, 2011.

[8]Miller, S. G., Paddock, A. F., Jegley, D. C., Grenoble, R. W., Guin, W. E., Jackson, J. R., and Segal, K. N. "Recertification and Equivalency and Test Results for IM7/8552-1 Following Extended Freezer Storage," 2018 SAMPE Conference.

[9]United Launch Alliance, "Delta IV Launch Services User's Guide", June 2013, URL: https://www.ulalaunch.com/docs/default-source/rockets/delta-iv-user's-guide.pdf [retrieved 19 November 2018].

[10]NASA Standard 5001-B., "Structural Design and Test Factors of Safety for Spaceflight Hardware," NASA Technical Standards Program, August 2016.

[11]Sleight, D. W., Satyanarayana, A., Li, Y., and Schultz, M. R., "Buckling Imperfection Sensitivity of Conical Sandwich Composite Structures for Launch-Vehicles, AIAA Sci-Tech 2018. AIAA 2018-1696.

[12]Anonymous, "Buckling of Thin-Walled Truncated Cones," NASA Space Vehicle Design Criteria, NASA SP-8019, September 1968.

[13]HyperSizer Structural Sizing Software, Collier Research Corp., Ver. 7.3.32, Hampton, VA, http://www.hypersizer.com, 2017.

[14] Hart-Smith, L. J., "Adhesive-Bonded Double-Lap Joints," Tech. Report, NASA CR-112235, 1973.

[15]MSC Nastran, MSC Software Corporation, Ver. 2016, Santa Ana, http://www.mscsoftware.com, 2016.

[16]Hoyt, D., Ward, S., & Minguet, P., "Strength and Fatigue Life Modeling of Bonded Joints in Composite Structures," American Society for Composites (ASC) 15th Technical Conference, 2000.

[17]Tong, L., "Strength of Adhesively Bonded Single-Lap and Lap-Shear Joints," International Journal of Solids and Structures, 35 (20), 2601-2616, 1997.

[18]Tong, L., "An Assessment of Failure Criteria to Predict the Strength of Adhesively Bonded Composite Double Lap Joints," *Journal of Reinforced Plastics and Composites,* 16, 699-713. 1997.

[19]Mason, B. H., Satyanarayana, A., and Sleight, D. W., "Test and Analysis Correlation for Sandwich Composite Longitudinal Joint Specimens," AIAA Sci-Tech 2019.